Microspectrofluorometry of the Protonation State of Ellipticine, an Antitumor Alkaloid, in Single Cells

Franck Sureau,* Francois Moreau,‡ Jean-Marc Millot,§ Michel Manfait,§ Béatrice Allard,¶ Jean Aubard,¶ and Marc-Antoine Schwaller¶

*Laboratoire de Physique et Chimie Biomoléculaire, CNRS URA 198, Institut Curie et Université Pierre et Marie Curie, 75005 Paris; ‡Laboratoire de Physiologie Cellulaire et Moléculaire, CNRS URA 1180, Université Pierre et Marie Curie, 75005 Paris; §Laboratoire de Spectroscopie Biomoléculaire, Faculté de Pharmacie, 51096 Reims Cedex; and ¶Institut de Topologie et Dynamique des Systèmes, CNRS URA 34, Université Paris 7, 75005 Paris, France

ABSTRACT The protonation state and intracellular distribution of ellipticine were investigated in single human mammary T47D cells by confocal laser microspectrofluorimetry. In the cell nucleus, only the protonated form of ellipticine was detected as a direct consequence of its apparent pK increase upon DNA binding. Both protonated and neutral forms were present in the aqueous cytoplasm, where the pH is close to the drug pK. When cells were incubated in high concentrations of K^+, a condition that depolarizes the plasma membrane potential, ellipticine cellular accumulation was reduced. In the cytoplasm, ellipticine was mainly bound to mitochondria, and its protonation equilibrium was shifted toward the neutral form. The fluorescence spectrum of ellipticine bound to mitochondria was insensitive to valinomycin, whereas it was markedly shifted toward the protonated form after carbonyl cyanide *p*-trifluoromethoxy-phenylhydrazone or nigericin addition. Similar studies with ellipticine bound to isolated mitochondria suggest that it behaves as a fluorescent probe of mitochondrial pH in both isolated mitochondria and single living cells.

INTRODUCTION

The pioneering study by Lermann on the mechanism of proflavine binding to DNA was the first to propose the intercalation model, which consists of the insertion of planar aromatic compounds between DNA base pairs (Lermann, 1961). Since this first description of the model, considerable research has been oriented toward the generalization of this drug-DNA binding mode to numerous other polycyclic planar molecules and to the understanding of its biological consequences, especially in pharmacology. Thus, some molecules in the series of anthracyclines, actinomycins, acridines, and ellipticines have been successfully used to treat human malignancies (Baguley, 1991). However, until now, the relationships between drug-DNA binding and antitumor activity have not been fully demonstrated. Moreover, the genuine subcellular target(s) of the drug, which induces the primary cytotoxicity, has not yet been fully established. Despite the high affinity of these molecules for DNA in vitro, several studies have shown that inside the cell, the available drugs were mainly located in the cytoplasm exhibiting a speckled distribution (Charcosset et al., 1983; Larsen et al., 1986; Auclair et al., 1988). This suggests that they are mainly localized within some cytoplasmic organelles. In addition, previous in vitro studies on isolated mitochondria have shown that anthracyclines (Goodmaghtigh et al., 1982; Porumb and Petrescu, 1986) and ellipticines (Dupont et al., 1987, 1990) behave as powerful metabolic inhibitors of oxidative phosphorylation. If a similar mitochondrial interaction could occur in an intact cell, it would cause severe changes in the cell's metabolism. Knowledge of the mechanisms governing the subcellular distribution of these drugs is therefore relevant to understanding their cytotoxic pathway. Antitumor drugs in the series of anthracyclines (Burke et al., 1987), acridines (Denny et al., 1987), or ellipticines (Dodin et al., 1988) are all weak bases, with pKs of protonation ranging between 7.4 and 8.5. Thus, inside the cell, these molecules exist in their two protonation states, namely the cationic protonated form and the neutral form. The protonation equilibrium can be shifted as a function of the interactions of these molecules with biological macromolecules (Dodin et al., 1990) or their accumulation in organelles, such as lysosomes and mitochondria, where a specific local pH exists (Rottenberg, 1989). In the present study, we investigated the relationships between the protonation state of antitumor alkaloids and their accumulation in different cell compartments, using ellipticine as the model. Ellipticine appeared to be a good candidate for such a study, since it displays a high fluorescence quantum yield, its pK of protonation (7.4) is close to the cytoplasmic pH, and its unprotonated (neutral) and protonated (cationic) forms exhibit specific fluorescence emission spectra. The patterns of ellipticine nuclear and cytoplasmic staining were examined in living T47D cells by means of confocal laser microspectrofluorometry. This technique was chosen for its high spatial and spectral resolution, which makes possible the simultaneous determination of drug's localization and protonation state. Fluorescence emission intensities and spectra recorded from different cell compartments were compared to those obtained in vitro when ellipticine was bound to isolated chromatin and mitochondria. Specific ionophores were used to investigate the respective influence of transmembrane $\Delta\psi$ and ΔpH on the drug protonation state.

Received for publication 24 March 1993 and in final form 30 July 1993.

Address reprint requests to Dr. Marc-Antoine Schwaller, Institut de Topologie et Dynamique des Systèmes, CNRS URA 34, Université Paris 7, 1, rue Guy de la Brosse, 75005 Paris, France.

0006-3495/93/11/1767/08 $2.00

MATERIALS AND METHODS

Chemicals

Ellipticine was a generous gift from Dr. E. Lescot (Institut Gustave Roussy, Villejuif, France). It was routinely checked for purity by both thin-layer chromatography and high-performance liquid chromatography. An aqueous stock solution of ellipticine (hydrochloride) was stored at −20°C and used within 2 weeks. Working solutions of the drug were prepared immediately before each experiment by diluting the stock solution, and then the drug concentration was determined by UV absorption.

Calf thymus DNA (highly polymerized sodium salt), carbonyl cyanide *p*-trifluoromethoxy-phenylhydrazone (FCCP), and nigericin were purchased from Sigma Chemical Co. (St. Louis, MO). DNA was dissolved in 0.01 M acetate buffer (pH 5) and sonicated for ~3 min at 4°C in order to reduce its viscosity. Sodium dodecyl sulfate and Triton X-100 were of the highest available grade and were used as such or after reprecipitation from water (except for Triton X-100) without any significant difference. The mitochondrial probe JC-1 was purchased from Molecular Probes (Eugene, OR).

Dimyristoyl phosphatidyl glycerol liposomes and dimyristoyl phosphatidyl choline liposomes were prepared and characterized as previously described (Aubard et al., 1990). For pK determinations, the following buffers were obtained from Merck: pH 5 (0.025 M acetate), pH 7 (0.025 M phosphate), pH 8 (0.025 M borate), pH 9 (0.025 M borate), pH 11 (0.025 M borate); mixtures of pH 9 and pH 11 were used to obtained various pHs within this range. NaCl was added to these buffers to obtain a final salt concentration of 0.1 M.

Cell culture

Human T47D mammary tumor cells, isolated from the pleural effusion fluids of a patient with breast carcinoma (Keydar et al., 1979), were obtained from Dr. H. Magdelenat (Institut Curie, Paris, France). The cells were grown as monolayers (25 cm^2 flasks) in RPMI 1640 with 10% fetal calf serum, L-glutamine (2 mM), and penicillin-streptomycin (50 IU/ml, 50 μg/ml, respectively), all purchased from Boehringer Mannheim (Meylan, France). The cells were maintained in a humidified atmosphere of 95% air/5% CO_2 at 37°C. Confluent cultures were used for all experiments.

Isolation of nuclei

Mouse leukemia L1210 cells, collected 7 days after passage into three DBA/2 mice were suspended, at 4°C, in 100 ml of a buffer containing 0.25 M sucrose and 5 mM EDTA (pH 8) and centrifuged for 5 min at 1500 × *g*. The cells were then washed twice in the same buffer and then homogenized in buffer containing Tris-HCl 10 mM (pH 8), 75 mM NaCl, 0.1 mM phenylmethylsulfonyl fluoride, and 26 mM EDTA. The homogenate was centrifuged at 1000 × *g* for 5 min, and the supernatant was discarded. The pellet was then suspended in the same buffer containing 0.25% (v/v) of Nonidet P40. The suspension was incubated at 4°C for 40 min, under gentle stirring, and centrifuged at 100 × *g* for 5 min. The nuclei were then washed 3 times in 0.35 M sucrose and 0.1 M EDTA (pH 8).

Chromatin isolation

The nuclei were resuspended in 10 mM Tris-HCl (pH 7.4), 40 mM NaCl, 3 mM $MgCl_2$, and 1 mM $CaCl_2$. Nuclei were digested at 37°C for 5 min in the presence of 150 units/ml micrococcal nuclease (Boehringer). The digestion was stopped by cooling to 4°C and the addition of EDTA to a final concentration of 10 mM. The digested nuclei were dialyzed for 12 h against a buffer containing 80 mM NaCl, 5 mM Tris-HCl (pH 7.4), and 0.2 mM EDTA. After homogenization, the suspension was centrifuged for 5 min at 800 × *g*, and the supernatant contained the soluble chromatin. The chromatin concentration was expressed as its DNA content, determined by its UV absorbance at 260 nm, assuming that 50 μg/ml of chromatin corresponds to an optical density of 1.1 at this wavelength. For drug binding experiments, the chromatin was dialyzed overnight at 4°C against 10 mM cacodylate buffer (pH 7.0), containing 0.2 mM EDTA and 10 mM NaCl, and further diluted in the same buffer to obtain a final concentration of ~300 μM as expressed in nucleotides.

Isolation of mitochondria

Rat liver mitochondria from male Wistar albino rats (150–200 g) were prepared by differential centrifugation through a medium containing 0.225 M mannitol, 0.075 M sucrose, 10 mM 4-(2-hydroxyethyl)-1-piperazine-ethanesulfonic acid (pH 7.2), 0.2 mM EDTA, and 0.1% bovine serum albumin. Rat liver (3 g) was cut into small pieces, ground in a potter homogenizer in 20 ml of medium at 4°C, and centrifuged at 750 × *g* for 10 min. The supernatant was centrifuged at 8700 × *g* for 10 min. The pellet was superficially washed twice with 10 ml of medium and centrifuged at 6000 × *g* for 10 min in order to remove the fluffy layer. The final pellet was suspended in 500 μl of ice-cold homogenization medium. The mitochondrial protein content was determined using the method of Lowry et al. (1951) and bovine serum albumin as the standard.

Fluorescence titration experiments

These experiments were performed using an LS 50 Perkin-Elmer spectrofluorometer, in quartz fluorescence cells (1-cm path length) containing 3 ml of buffered solution. Before titration, excitation and emission spectra of the drug in the absence and the presence of an excess of either chromatin or mitochondria were recorded. Addition of DNA, chromatin, or mitochondria to a solution of ellipticine led to a marked increase in fluorescence intensity associated with a shift toward the red end of the excitation spectrum (Schwaller et al., 1989). The amount of ellipticine bound to macromolecules or mitochondria (C_b) was calculated from the increase of the fluorescence emitted by the ellipticine chromophore upon binding, according to the following equation:

$$C_b = [\Delta I_f / k(V - 1)],$$

where ΔI_f is the difference between the fluorescence intensities emitted by free and bound ellipticine, V is the ratio of the fluorescence quantum yield of bound to free drug at 520 nm, and k is a factor that converts free drug concentration to fluorescence intensities.

Values of r, the ratio of bound ellipticine to chromatin or mitochondriae concentrations, and C, the free drug concentration calculated from binding experiments, were analyzed routinely according to Scatchard's equation (Scatchard, 1949):

$$r/C = K(n - r)$$

where K (given by the slope of the Scatchard plot) represents the ellipticine association constant to an isolated site and n (given by the intercept of the r-axis) represents the maximum number of ellipticine molecules bound per nucleotide (in DNA or chromatin binding experiments) or per phospholipid (in the case of mitochondria), assuming that rat liver mitochondria contain 200 nmol phospholipids/mg protein (Rottenberg, 1984).

Microspectrofluorometry

The UV-visible confocal laser microspectrofluorometer prototype was built around a Zeiss UMSP 80 UV epifluorescence microscope (Carl Zeiss, Inc., Oberkochen, Germany), optically coupled by UV reflecting mirrors to a Jobin-Yvon HR640 spectrograph (ISA, Longjumeau, France) (Sureau et al., 1990). The 351-nm UV line of an argon laser (model 2025; Spectra-Physics, Mountain View, CA) was used for drug excitation. The diameter of the laser beam is first enhanced through a double-lens beam expander in order to cover the entire numerical aperture of the microscope's optics. The laser beam is then deflected by the epi-illumination system (dichroic mirror or semireflecting glass) and focused on the sample through the microscope objective (×63 Zeiss Neofluar water-immersion objective; numerical aperture = 1.2) on a circular spot 0.5 μm in diameter. The excitation power

is reduced to less than 0.1 μW by neutral optical density filters. The objective was immersed in the culture medium, and a circular area 0.8 μm in diameter was selected at the sample level, by interposing a field diaphragm on the emission pathway of the microscope, to selectively collect the fluorescence signal from the nucleus or a specific cytoplasmic area. Confocal conditions are met when the image of this analysis field diaphragm through the microscope objective perfectly coincides with the focus of the laser beam on the sample. Under these conditions, the experimental spatial resolution, measured on calibrated latex beads (2, 0.6, and 0.16 μm in diameter) labeled with the fluorescent probe fluorescein, is 0.5 μm for the directions *X*, *Y*, and *Z*. Finally the fluorescence spectra were recorded after spectrograph dispersion, in the 380–630 region on a 1024 diode-intensified optical multichannel analyzer (Princeton Instruments, Inc., Princeton, NJ) with a resolution of 0.25 nm/diode. Each fluorescence emission spectrum was collected for 1 to 10 s. Data were stored and processed on an 80286 IBM PS/2 microcomputer using the Jobin-Yvon "Enhanced Prism" software. It should be noted that, in order to avoid any possible fluorescence from a plastic or glass support during analysis with near-UV excitation, cells were grown on quartz plates that were then placed on the microscope stage in 50-mm thermostated Petri dishes, filled with 5 ml of phosphate-buffered saline. A uranyl glass bar was used as a fluorescence standard to control laser power and instrumental response and to enable quantitative comparison between spectra recorded on different days. Sample heating, photobleaching, and photodamage were assessed empirically and found to be negligible under our experimental conditions. In particular, cells always remained viable after repeated fluorescence determinations, as controlled by phase-contrast microscopy.

Fluorescence image of JC-1-stained T47D cells

JC-1 is a carbocyanine cationic dye that can be exploited for imaging live mitochondria on the stage of a microscope. It has an advantage over rhodamines and other carbocyanines in that its color changes reversibly from green to red in response to the membrane potential of energized mitochondria (Reers et al., 1991; Smiley et al., 1991). Photomicrographs of stained mitochondria in cells were obtained with the microspectrofluorimeter system hooked up to an Olympus OM2 camera, using a 50-W mercury arc lamp for JC-1 excitation and the appropriate filters: Zeiss barrier (LP 520 nm), dichroic mirror (FT 510 nm), and exciter (450–490 nm), as previously described (Smiley et al., 1991). Fluorescent images were recorded on 400 ASA Ektachrome positive film and printed on Konica paper.

RESULTS

Protonation state of ellipticine free or bound to DNA, chromatin, model membranes, or mitochondria

Ellipticine can be protonated at its N(2) nitrogen atom (see chemical formula). The unprotonated (neutral) form of ellipticine presents a characteristic UV absorption band at 290 nm and a typical emission band at 430 nm, whereas the cationic (protonated) form of the drug shows an absorption band peaking at 310 nm and an emission band at 520 nm (Fig. 1). The pK of protonation of the drug can be determined from either absorption (ratio of absorbances at 290/310 nm versus pH) or fluorescence spectroscopy (ratio of emissions at 430/520 nm versus pH). As shown in Table 1, the intrinsic protonation pK (pK_i) of ellipticine in water is 7.4. When ellipticine was bound to neutral hydrophobic structures, such as Triton X-100 micelles or zwitterionic liposomes (dimyristoyl phosphatidyl choline liposomes), its pK_{app} was ~6 as a result of the reduced polarity at the interface, as previously described for other lipoid pH indicators (Mukerjee and Banerjee, 1964; Fernandez and Fromhertz, 1977). By contrast, when ellipticine was bound to anionic macromolecules such as dimyristoyl phosphatidyl glycerol liposomes or DNA, its apparent pK (pK_{app}) was increased to ~9. These pK_{app} increases can be interpreted as resulting from an enhanced proton activity at the anionic interface (Fernandez and Fromhertz, 1977) according to Boltzmann's law:

$$a_i = a_w \exp(-F\Delta\psi/RT)$$

where a_w is the proton activity in the bulk water, $\Delta\psi$ is the interfacial potential, R is the general gas constant, F is Faraday's constant, and T is the temperature in °K. The apparent pK is then given by the following expression (Fernandez and Fromhertz, 1977):

$$pK_{app} - pK_i = -F\Delta\psi/2.3RT.$$

The apparent pK of ellipticine bound to chromatin, as compared to pure DNA, was lower (pK_{app} = 8.5 and 9.1, respectively) (Fig. 2). This effect can also be interpreted taking into account the partial neutralization of the DNA/water interface by lysine-rich histones (Larue et al., 1987). When bound to mitochondria, the ellipticine pK_{app} was ~7.5 (Table 1), which suggests that the ellipticine binding domain in the membrane is composed of a mixture of both neutral (pK_{app} ~6) and anionic phospholipids (pK_{app} ~9).

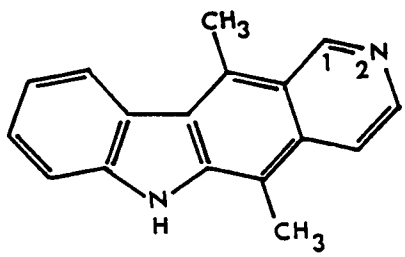

Chemical formula of ellipticine

SCHEME I

Binding to DNA, chromatin, and mitochondria

As previously described for ellipticine, its derivatives, and other DNA-intercalating drugs, it is expected that free molecules in aqueous solution and those bound to DNA (Schwaller et al., 1989), chromatin (Larue et al., 1987), or model membranes (Aubard et al., 1990) will have different fluorescence properties. Accordingly, the addition of DNA, chromatin, or mitochondria to a solution of ellipticine led to a marked increase in fluorescence intensity. The increased fluorescence emitted as a function of ellipticine binding, expressed as the ratio of the intensities of bound to free fluorescence, was estimated from extrapolation of a double-reciprocal plot of fluorescence increase versus macromolecule concentration as shown in Fig. 3 for binding to mitochondria. The ratio of fluorescence intensities obtained for ellipticine bound to DNA, chromatin, or mitochondria over free ellipticine are given in Table 1. The Scatchard plot ob-

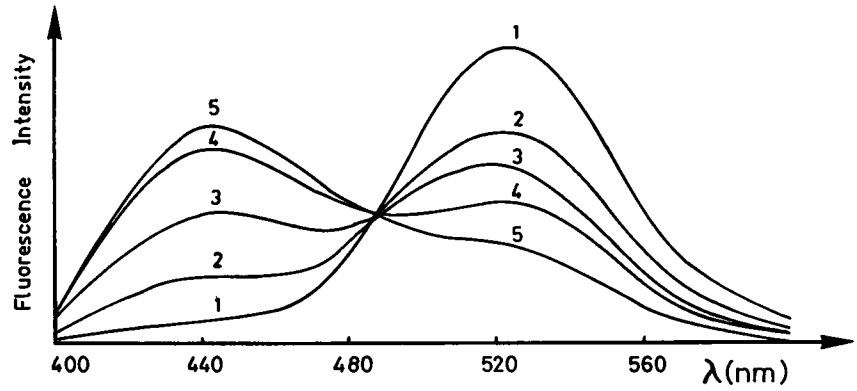

FIGURE 1 Fluorescence emission spectra of an aqueous solution of ellipticine at the following pH values (25°C): (*1*) pH = 6.0; (*2*) 7.4; (*3*) 8.9; (*4*) 11.2; (*5*) 12.2. Excitation wavelength, 290 nm.

TABLE 1 Apparent pK and binding parameters of ellipticine with various macromolecules

Macromolecules	pK_{app}*	V‡	K (10^6 M^{-1})§	n‖
H_2O	7.4	1		
CT-DNA	9.1	17		
Chromatin	8.5	16	1.6¶	0.05¶
DMPG liposomes	9.2			
DMPC liposomes	6.2			
SDS micelles	9.4			
Triton X-100 micelles	6.1			
Mitochondria	7.5	11	2.0	0.05

DMPG, dimyristoyl phosphatidyl glycerol; DMPC, dimyristoyl phosphatidyl choline; SDS, sodium dodecyl sulfate; CT-DNA, calf thymus DNA.
*The pK of protonation was estimated from the absorbance ratio at 290 and 310 nm and from the fluorescence ratio at 430 and 520 nm (experimental conditions are described in Materials and Methods).
‡*V*, ratio of fluorescence intensities of bound/free ellipticine at 520 nm.
§*K*, association constant.
‖*n*, number of ellipticine molecules bound per nucleotide or phospholipid was determined as described in Materials and Methods.
¶Binding constants were estimated from the binding curve at a low drug:phosphate ratio (high-affinity binding sites).

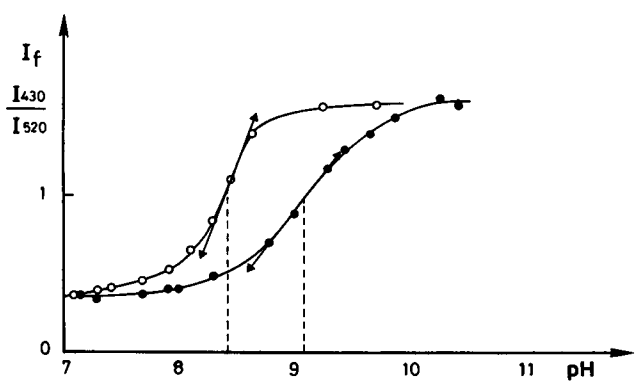

FIGURE 2 Variation of the ellipticine I_{430}/I_{520} fluorescence ratio with pH in the bulk phase in the presence of an excess (100 μM as expressed in nucleotide) of either CT-DNA (●) or chromatin (○).

tained when titrating a fixed amount of chromatin with ellipticine is shown in Fig. 4 *a*. The binding curve indicates the presence of two types of binding sites and a positive cooperative binding process at a low drug:chromatin ratio, as previously described for ellipticines and other DNA-

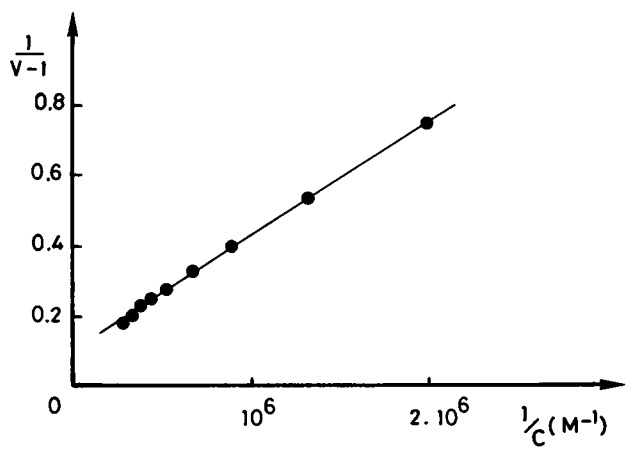

FIGURE 3 Ratio of the fluorescence intensities of mitochondrial-bound to free ellipticine measured at 520 nm in anaerobic medium containing 250 mM sucrose, 5 mM 4-morpholinepropanesulfonic acid (MOPS) (pH 7.4), 5 mM $MgCl_2$, and 5 mM succinate.

intercalating drugs (Auclair et al., 1988; Larue et al., 1987); initial binding to the linker region induces DNA unwinding with partial unwraping of DNA from the core histone, which increases the available number of binding sites. From the slope of the titration curve obtained at a low drug:nucleotide ratio, an association constant of 1.6×10^6 M^{-1} can be calculated. For ellipticine binding to mitochondria, the titration curve was linear (Fig. 4 *b*), indicating a single class of binding sites without any cooperative processes. From this titration curve were calculated an association constant of $\sim 2 \times 10^6$ M^{-1} and a maximum number of bound ellipticine molecules per phopholipid of ~0.05. These binding parameters (Table 1) are close to those previously inferred from the binding of ellipticine derivatives to model membranes (Aubard et al., 1990).

Cytofluorescence localization of ellipticine in T47D cells

To study the intracellular distribution of ellipticine, T47D cells were incubated in the presence of 0.5 μM ellipticine for 1 h. An incubation with 1 μM ellipticine for 48 h reduced the viability of this cell line to 50%. Ellipticine fluorescence

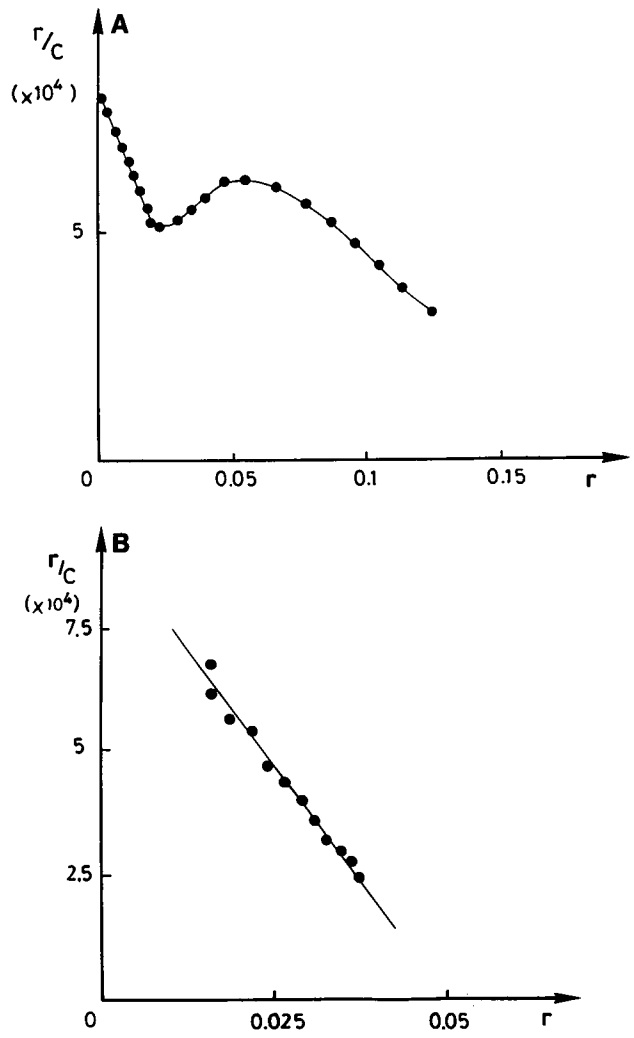

FIGURE 4 Scatchard isotherms for the binding of ellipticine to chromatin (*a*) or energized mitochondria (*b*). (*a*) 10 mM cacodylate buffer, 0.1 M NaCl (pH 7.4). (*b*) aerobic medium containing 250 mM sucrose, 5 mM MOPS (pH 7.4), 5 mM $MgCl_2$, and 5 mM succinate.

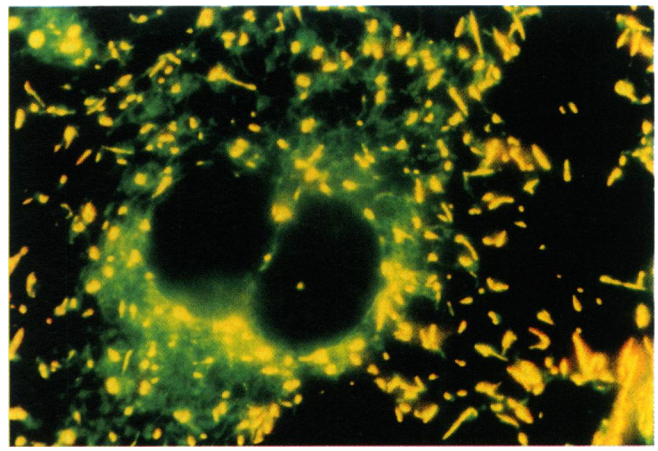

FIGURE 5 Epifluorescence micrograph of the localization of JC-1 in T47D cells. The yellow emission corresponds to J-aggregate fluorescence and the green emission corresponds to JC-1 monomer fluorescence. Experimental conditions are described in Materials and Methods.

was principally located in the cytoplasm, and a weaker fluorescence emanated from the nucleus. Moreover, using different cell lines, it was previously shown that, in the cytoplasm, ellipticine fluorescence was mainly localized in granular structures (Charcosset et al., 1983; Larsen et al., 1986; Auclair et al., 1988). Taking into account that ellipticine interacts strongly with mitochondria in vitro (Dupont et al., 1987, 1990), we tentatively analyzed the ability of ellipticine to localize at the level of intracellular mitochondria. To measure the specific fluorescence emission spectrum of ellipticine interacting with mitochondria, T47D cells were preincubated with JC-1, a specific energy potential-dependent mitochondrial fluorescent probe (Reers et al., 1991; Smiley et al., 1991) that forms red fluorescent J-aggregates when it accumulates in mitochondria. Thus, a mitochondriae localization (Fig. 5) was first observed by fluorescence imaging at 490 nm (see Materials and Methods). The 351-nm laser line, used for ellipticine excitation, was then focused in the cytoplasm either in the cytosol or in mitochondria, and the corresponding fluorescence spectra were recorded (see below).

Fluorescence emission of ellipticine from three different cell compartments

The ellipticine protonation state was analyzed in three different cell compartments of T47D cells using confocal laser microspectrofluorometry; the emission spectrum from a selected microvolume within the cell nucleus presented a single band centered at 520 nm (Fig. 6, *spectrum 2*). This single band, which characterizes the emission of the protonated cationic form of the drug (cf. Fig. 1), was identical to the emission band recorded from DNA-bound ellipticine (Fig. 6, *spectrum 3*), suggesting that, in the cell nucleus, the drug binds to DNA, in its cationic state, as would be expected from

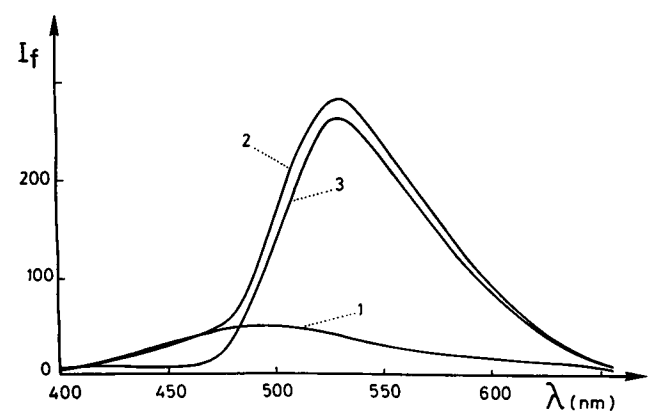

FIGURE 6 Microspectrofluorometric spectra emitted from a selected microvolume of the T47D cell nucleus before (*spectrum 1*) and after incubation with 0.5 μM ellipticine for 5 h (*spectrum 2*) and comparison with the fluorescence emission spectrum of ellipticine bound to CT-DNA (DNA/ellipticine = 100) (*spectrum 3*). Experimental conditions are described in Materials and Methods.

its apparent pK for isolated DNA and chromatin (Table 1). When the laser beam was focused in cytosol, the emission spectrum (corrected for cell intrinsic fluorescence) consisted of two bands centered at ~430 and 520 nm, respectively (Fig. 7, *spectrum 1*), with an intensity ratio (I_{520}/I_{430}) of ~3. These two bands are characteristic of the neutral (blue band) and protonated (green band) forms, which suggested that the drug existed in its two protonation states in the cytosol, as would be expected from the pH of this cell compartment. Cells were also incubated in medium containing high concentrations of K^+, to specifically collapse the plasma membrane potential (Andrews et al., 1991). Under these conditions, the cytosolic fluorescence intensity decreased, essentially because of a decrease in the protonated form to approximately one-third of its initial value (Fig. 7, *spectrum 2*). This observation confirms that the distribution of the protonated form between cytosol and external medium is governed by the plasma membrane potential, as previously described with ellipticinium derivatives (Charcosset et al., 1984; Sautereau and Trombe, 1986). When the laser beam was focused on mitochondria, a fourfold increase of the whole fluorescence intensity (relative to cytosol) was observed (Fig. 8, *spectrum 1*). Moreover, the ratio (I_{520}/I_{430}) of the two specific fluorescence bands was markedly decreased to ~1. The relative enhancement of the blue emission band revealed that, in this area, the ellipticine protonation equilibrium was shifted toward the neutral form. Since the pH of the whole cytosol was buffered near neutrality, the only subcellular compartment displaying alkaline conditions and in which ellipticine might have accumulated was the inner mitochondrial membrane-matrix interface (Dupont et al., 1990; Rottenberg, 1989). To confirm this hypothesis, intracellular fluorescence spectra were recorded in the presence of specific mitochondrial ionophores. When T47D cells were incubated with 5 μM FCCP, a protonophore that specifically collapses the mitochondrial proton electrochemical gradient ($\Delta\mu H+$) (Johnson et al., 1981), the I_{520}/I_{430} ratio was markedly increased (Fig. 8, *spectrum 2*). This observation suggests that the blue emission band of ellipticine was mainly associated with energized mitochondria. To determine whether the change in ellipticine fluorescence bound to energized mitochondria was due to the $\Delta\psi$ or to the ΔpH component of the proton electrochemical gradient, cells were incubated with the ionophore valinomycin to specifically investigate the influence of the mitochondrial membrane potential. Valinomycin is a K^+ ionophore that slightly hyperpolarizes the plasma membrane but depolarizes the mitochondrial membrane potential (Johnson et al., 1981). When 2 μM valinomycin was added to T47D cells loaded with ellipticine, the I_{520}/I_{430} ratio was unaffected (Fig. 8, *spectrum 3*). The ionophore nigericin induces an electrically neutral exchange of protons for potassium ions and results in the dissipation of the pH gradient across the mitochondrial membrane (Davies et al., 1985). When nigericin (5 μg/ml) was added, the I_{520}/I_{430} ratio was increased to ~0.8 (Fig. 8, *spectrum 4*). Thus, the ΔpH appears to be responsible for the specific protonation state of ellipticine bound to mitochondria. The fluorescence spectra obtained from mitochondria within the cell were compared to those obtained when ellipticine was bound to isolated rat liver mitochondria resuspended in an aerobic buffer with succinate as the respiratory substrate (Fig. 9). Addition of nigericin to the suspension induced a shift of the protonation equilibrium toward the cationic form (Fig. 9, *spectrum 3*). This last observation confirmed that ellipticine behaves as a fluorescent probe of mitochondrial pH both in vitro in isolated organelles and in single living cells.

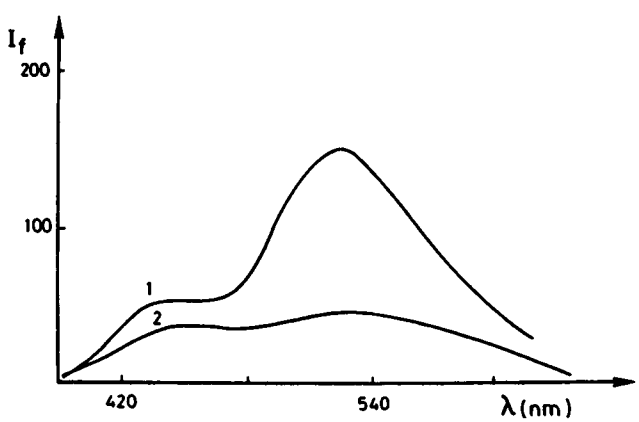

FIGURE 7 Effect of the potassium concentration on ellipticine fluorescence emitted from a selected microvolume of T47D aqueous cytoplasm. Spectra were corrected for intrinsic fluorescence emitted from aqueous cytoplasm before drug incubation (0.5 μM ellipticine for 5 h). Spectrum 1, 5 mM KCl; spectrum 2, 50 mM KCl.

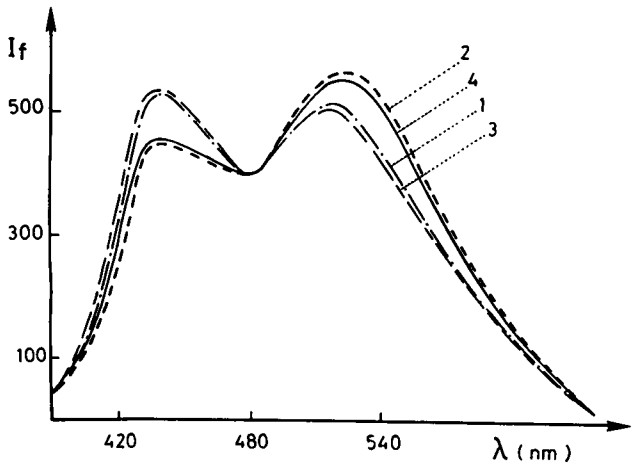

FIGURE 8 Effect of FCCP, valinomycin, and nigericin on the ellipticine fluorescence spectrum emitted from mitochondria in T47D cell cytoplasm. Spectra were corrected for the intrinsic fluorescence before drug incubation (0.5 μM ellipticine for 5 h). The laser was focused on mitochondria before (*spectrum 1*) and after the addition of FCCP (*spectrum 2*), valinomycin (*spectrum 3*), or nigericin (*spectrum 4*).

DISCUSSION

The importance of the plasma membrane potential in the cellular uptake and retention of charged ellipticines has previously been reported in both prokaryotic and eukaryotic cell

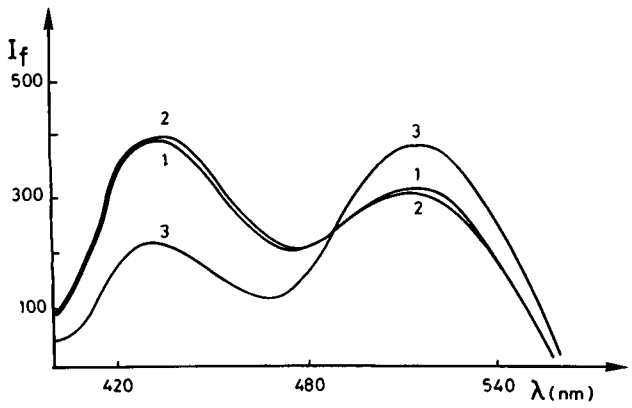

FIGURE 9 Effect of the dissipation of the transmembrane ΔpH by nigericin on the fluorescence emission of ellipticine bound to isolated mitochondria energized by succinate. Mitochondria (0.25 mg/ml) were suspended in aerobic medium containing 250 mM sucrose, 5 mM MOPS (pH 7.4), 5 mM $MgCl_2$, and 5 mM succinate and incubated with 0.5 μM ellipticine for 5 min. The fluorescence emission spectrum (λ_{exc} = 300 nm) was recorded before (*spectrum 1*) and after the addition of valinomycin (*spectrum 2*) or nigericin (*spectrum 3*).

lines (Sautereau and Trombe, 1986; Charcosset et al., 1984). A similar relationship between a drug's cationic charge and its increased cellular accumulation and cytotoxicity has been demonstrated within the anthracycline (Burke et al., 1987) and rhodamine series (Lampidis et al., 1989; Lampidis et al., 1990). Our data obtained with ellipticine are in agreement with these results, since dissipation of the plasma membrane potential of T47D cells led to a marked decrease in ellipticine fluorescence detected in the cytosol, especially for the cationic form. These results suggest that the protonated form of ellipticine is sufficiently lipophilic and its positive charge is sufficiently delocalized to allow the drug to passively cross the plasma membrane and to accumulate in response to the negative membrane potential. Within the cell, ellipticine is present, as expected, in its two protonation states. Meanwhile, the drug's protonation equilibrium is highly dependent on its subcellular localization. In the nucleus, the drug's protonation equilibrium was shifted toward the protonated form, as noted when it is bound to isolated DNA (pK_{app} ~9.1) and chromatin (pK_{app} ~8.5). This observation suggests that ellipticine indeed reaches the cell nucleus where it binds, in its protonated form. Moreover, it indicates that the apparent interfacial proton activity is higher in nuclear DNA and chromatin than in cytosol. It would be interesting to consider this parameter in drug-DNA complex models in designing DNA-interacting anticancer drugs. Whereas it is generally thought that the main pharmacological target of ellipticine is nuclear DNA (Le Pecq et al., 1974; Auclair, 1987), our new data show that a large fraction of the drug remains in the cytoplasm, where it exists in its two protonation states. In the cytosol, neutral and cationic forms are detected in approximately equal proportions, as would be expected from the drug's intrinsic pK in water. This finding suggests that, in this compartment, the drug remains essentially free in solution and does not interact with neutral or charged macromolecules, which would lead to a shift in its pK_{app}, as observed in vitro (Table 1). In mitochondria, the drug colocalized with JC-1 and its protonation equilibrium was shifted toward the neutral form. Comparison of the effects of mitochondrial ionophores on the isolated organelles and those in situ in the cytoplasm of T47D cells suggests that ellipticine behaves as a fluorescent probe of the mitochondrial ΔpH both in vitro and in single living cells. From equilibrium-binding studies with isolated mitochondria (Fig. 4 *b*, Table 1), it appears that the binding of ellipticine to mitochondria is essentially a membrane interaction with binding parameters similar to those observed with artificial membrane models (Aubard et al., 1990) (association constant in the range of 10^6 M^{-1} and a maximal binding ratio of approximately one molecule to 20 phospholipids). If ellipticine had accumulated in the aqueous mitochondrial matrix space, it could probably bind to mitochondrial DNA, and as a consequence, its protonation equilibrium would be shifted toward the protonated form, a hypothesis that is inconsistent with our data. Moreover, it has previously been shown that, whereas ellipticine behaved as a potent inducer of nuclear auxotrophic mutations in yeast, it was ineffective in the mitochondrial "petite" mutation assay, even at concentrations as high as 80 μM (Pinto et al., 1982). These data suggest that, instead of accumulating in the mitochondrial matrix, ellipticine remains mainly localized in the inner membrane, facing the matrix. At this site, bound ellipticine behaves as a local pH probe, sensitive to changes in the interfacial proton activity resulting from mitochondrial respiration. This interpretation is consistent with recent bioenergetic data which suggested that the electrogenic H^+ ion movement involved in the rise of $\Delta\psi$, which occurs during the energy coupling in mitochondria, does not equilibrate with the bulk aqueous phases on either side of the mitochondrial membrane but is essentially localized within the domain of the inner membrane (McKenzie et al., 1991). In light of these observations, it is likely that the biological effects of ellipticine binding to mitochondria are attributable to biophysical and biochemical interactions with the inner membrane rather than an interaction with mitochondrial DNA. Indeed, previous studies on isolated mitochondria have shown that the interaction of ellipticine and derivatives with the inner membrane uncouples oxidative phosphorylation and inhibits the electron pathway at the level of cytochrome *c* oxidase (Dupont et al., 1987, 1990). Our data confirm that, in intact living cells, ellipticine interacts with mitochondria. This raises the possibility that, in addition to nuclear DNA, mitochondria could be one of the potential targets involved in the drug's cytotoxicity mechanism. When comparing fluorescence intensities detected in nuclei and mitochondria (Figs. 6 and 8), corrected for their respective fluorescence increases inferred from in vitro studies (Table 1), one can calculate that, at equilibrium, the drug fraction bound to mitochondria is slightly higher than that bound to chromatin. Accordingly, Scatchard analysis shows that the affinity of ellipticine for mitochondrial phospholipids is slightly higher than that for DNA base pairs in chromatin (Fig. 4 and Table 1). Since the mitochondrial volume

is very small compared to the cytosolic volume, it is difficult to definitively determine the local drug concentration, and the intracellular measurements can only be interpreted qualitatively. Finally, it can be emphasized that, during its transport from the external medium to the nucleus, the drug may interact with its mitochondrial target before reaching nuclear DNA. In light of these observations, it is more likely that ellipticine cytotoxicity is primarily due to its antimitochondrial activity.

REFERENCES

Andrews, P. A., S. C. Mann, H. H. Huynh, and K. D. Albright. 1991. Role of Na^+, K^+ ATPase in the accumulation of *cis*-diaminedichloroplatinum (II) in human ovarian carcinoma cells. *Cancer Res.* 51:3677–3681.

Aubard, J., P. Lejoyeux, M. A. Schwaller, and G. Dodin. 1990. Spectroscopy and kinetics of the interaction of ellipticinium derivatives with liposomes. Influence of aliphatic side-chain on the binding mechanism. *J. Phys. Chem.* 94:1706–1712.

Auclair, C. 1987. Multimodal action of antitumor agents on DNA: the ellipticine series. *Arch. Biochem. Biophys.* 259:1–14.

Auclair, C., M. A. Schwaller, B. Rene, H. Banoun, J. M. Saucier, and A. K. Larsen. 1988. Relationships between physicochemical and biological properties in a series of oxazolopyridocarbazole derivatives (OPCd); comparison with related antitumor agents. *Anti-Cancer Drug Design.* 3:133–144.

Baguley, B. C. 1991. DNA intercalating anti-tumour agents. *Anti-Cancer Drug Design.* 6:1–35.

Burke, T. G., M. J. Morin, A. C. Sartorelli, P. E. Lane, and Tritton, P. R. 1987. Function of the anthracycline amino group incellular transport and cytotoxicity. *Mol. Pharmacol.* 31:552–556.

Charcosset, J. Y., B. Salles, and A. Jacquemin-Sablon. 1983. Uptake and cytofluorescence localization of ellipticine derivatives in sensitive and resistant Chinese hamster lung cells. *Biochem. Pharmacol.* 32:1037–1044.

Charcosset, J. Y., A. Jacquemin-Sablon, and J. B. Le Pecq. 1984. Effect of membrane potential on the cellular uptake of 2-*N*-methyl-ellipticinium by L1210 cells. *Biochem. Pharmacol.* 33:2271–2275.

Davies, S., M. J. Weiss, J. R. Wong, T. J. Lampidis, and L. B. Chen. 1985. Mitochondrial and plasma membrane potentials cause unusual accumulation of rhodamine 123 by human breast adenocarcinoma-derived MCF-7 cells. *J. Biol. Chem.* 260:13844–13850.

Denny, W., A., G. J. Atwell, G. W. Rewcastle, and B. C. Baguley. 1987. Potential antitumor agents: 5-substituted derivatives of *N*-2-dimethylamino(ethyl)-9-aminoacridine-4-carboxamide with "in vivo" solid-tumor activity. *J. Med. Chem.* 30:658–653.

Dodin, G., M. A. Schwaller, J. Aubard, and C. Paoletti. 1988. Binding of ellipticine base and ellipticinium cation to calf-thymus DNA. A thermodynamic and kinetic study. *Eur. J. Biochem.* 176:371–375.

Dodin, G., J. Aubard, and M. A. Schwaller. 1990. Acid-base properties of ellipticine bound to DNA, micelles and liposomes. *Anti-Cancer Drug Design.* 5:129–134.

Dupont, J., G. Dodin, and M. A. Schwaller. 1987. Interactions between ellipticine derivatives and the mitochondrial respiratory chain. *Plant Sci. Lett.* 54:109–115.

Dupont, J., M. A. Schwaller, and G. Dodin. 1990. Short-term inhibitory interaction of ditercalinium with electron transport in isolated mammalian mitochondria. *Cancer Res.* 50:7966–7972.

Fernandez, M. S., and P. Fromhertz. 1977. Lipoid pH indicators as probes of electrical potential and polarity in micelles. *J. Phys. Chem.* 81:1755–1761.

Frakas, D. L., M. D. Wei, P. Febbroriello, J. H. Carson, and L. M. Loew. 1989. Simultaneous imaging of cell and mitochondrial membrane potential. *Biophys. J.* 56:1053–1069.

Goodmaghtigh, E., R. Brasseur, and J. M. Ruysschaert. 1982. Adriamycin inactivates cytochrome *c* oxidase by exclusion of the enzyme from its cardiolipin essential environment. *Biochem. Biophys. Res. Commun.* 104: 314–320.

Johnson, L. V., M. L. Walsh, B. J. Bockus, and L. B. Chen. 1981. Monitoring of relative mitochondrial membrane potential in living cells by fluorescence microscopy. *J. Cell Biol.* 88:526–535.

Keydar, I., L. Chen, S. Karby, F. R. Weiss, S. K. Yang, and H. V. Gelboin. 1979. Establishment and characterization of a cell line of human breast carcinoma origin. *Eur. J. Cancer.* 15:659–670.

Lampidis, T. J., C. Castello, A. D. Giglio, B. C. Pressman, P. Viallet, K. W. Trevorrow,, G. K. Valet, H. Tapiero, and N. Savaraj. 1989. Relevance of the chemical charge of rhodamine dyes to multiple drug resistance. *Biochem. Pharmacol.* 38:4267–4271.

Lampidis, T. J., N. Savaraj, G. K. Valet, K. Trevorrow, A. Fourcade, and H. Tapiero. 1990. Relationship of chemical charge of anticancer agents to increased accumulation and cytotoxicity in cardiac and tumor cells: relevance to multidrug resistance. *J. Cell. Pharmacol.* 1:16–22.

Larsen, A. K., J. Paoletti, J. R. Belehradek, and C. Paoletti. 1986. Uptake, cytofluorescence and cytotoxicity of oxazolopyridocarbazoles in murine sarcoma cells. *Cancer Res.* 46:5236–5241.

Larue, L., M. Quesne, and J. Paoletti. 1987. Interaction of an intercalating antitumoral agent: 9-hydroxy-2-methyl ellipticinium with chromatin. *Biochem. Pharmacol.* 36:3563–3569.

Le Pecq, J. B., D. X. Nguyen, C. Gosse, and C. Paoletti. 1974. A new antitumoral agent: 9-hydroxyellipticine. Possibility of a rational design of anticancerous drugs in the series of DNA intercalating drugs. *Proc. Natl. Acad. Sci. USA.* 71:5078–5082.

Lermann, L. S. 1961. Structural considerations on the interaction of DNA and acridines. *J. Mol. Biol.* 3:18–24.

Lowry, O. H., N. J. Rosebrough, A. L. Farr, and R. J. Randall. 1951. Protein measurement with the Folin phenol reagent. *J. Biol. Chem.* 193:265–275.

McKenzie, R. J., G. F. Azzone, and T. E. Conover. 1991. Bulk phase proton fluxes during the generation of membrane potential in rat liver mitochondria. *J. Biol. Chem.* 266:803–809.

Mukerjee, P., and K. Banerjee. 1964. A study of the surface pH of micelles using solubilized indicator dyes. *J. Phys. Chem.* 68:3567–3574.

Pinto, M., M. Guerineau, and C. Paoletti. 1982. Mitochondrial and nuclear mutagenicity of ellipticine and derivatives in yeast *Saccharomyces cerevisiae. Biochem. Pharmacol.* 31:2161–2167.

Porumb, H., and I. Petrescu. 1986. Interaction with mitochondria of the anthracycline cytostatics adriamycin and daunomycin. *Prog. Biophys. Mol. Biol.* 48:103–109.

Reers, M., T. W. Smith, and L. B. Chen. 1991. J-aggregate formation of a carbocyanine as a quantitative fluorescent indicator of membrane potential. *Biochemistry.* 30:4480–4486.

Rottenberg, H. 1984. Membrane potential and surface potential in mitochondria. *J. Membr. Biol.* 81:127–138.

Rottenberg, H. 1989. Proton electrochemical potential gradient in vesicles, organelles and prokaryotic cells. *Methods Enzymol.* 172:63–85.

Sautereau, A. M., and M. C. Trombe. 1986. Electric transmembrane potential mutation and resistance to cationic and amphiphilic antitumoral drugs derived from pyridocarbazole, 2-*N*-methyl ellipticinium and 2-*N*-methyl-9-hydroxy ellipticinium, in *Streptococcus pneumoniae. J. Gen. Microbiol.* 132:2637–2641.

Scatchard, G. 1949. The attraction of proteins for small molecules and ions. *Ann. N.Y. Acad. Sci.* 551:660–666.

Schwaller, M. A., J. Aubard, C. Auclair, C. Paoletti, and G. Dodin. 1989. The GC base-pair preference of 2-*N*-methyl-9-hydroxy ellipticinium. *Eur. J. Biochem.* 181:129–134.

Smiley, S. T., M. Reers, C. Mottola-Hartshorn, M. Lin, A. Chen, T. W. Smith, G. D. Steele, Jr., and L. B. Chen. 1991. Intracellular heterogeneity in mitochondrial membrane potentials revealed by J-aggregate-forming lipophilic cation JC-1. *Proc. Natl. Acad. Sci. USA.* 88:3671–3675.

Sureau, F., L. Chinsky, M. Duquesne, A. Laigle, P. Y. Turpin, C. Amirand, J. P. Ballini, and P. Vigny. 1990. Microspectrofluorometric study of the kinetics of cellular uptake and metabolization of benzo(*a*)pyrene in human T47D mammary tumor cells: evidence for cytochrome P_{1-450} induction. *Eur. Biophys. J.* 18:1707–1713.